Re-irradiation of silver nanoparticles obtained by laser ablation in water and assessment of their antibacterial effect

M. Fernández-Arias[a]*, M. Boutinguiza[a], J. del Val[a], E. Medina[b], D. Rodríguez[b], A. Riveiro[a], R. Comesaña[c], F. Lusquiños[a], F.J. Gil[d] , J. Pou[a]

[a] Applied Physics Dpt., University of Vigo, EEI, Lagoas-Marcosende, Vigo, E-36310, Spain

[b] Biomaterials, Biomechanics and Tissue Engineering Group, Materials Science and Metallurgical Engineering Dept., UPC-Barcelona TECH, Sant Adrià del Besòs, Barcelona, E-08930, Spain

[c] Materials Eng., Applied Mech., and Construction Dpt., University of Vigo, Lagoas-Marcosende, E-36310, Vigo, Spain

[d] School of Dentistry. Universitat Internacional de Catalunya, Barcelona, Spain

*Corresponding author at: Applied Physics Dpt., University of Vigo, EEI, Lagoas-Marcosende, Vigo, E-36310, Spain. Tel.: +34986812216; fax: +34986812201.

E-mail address: monfernandez@uvigo.es (M. Fernández-Arias)

ABSTRACT

The rapid evolution of resistant bacteria is a huge problem in medicine because makes the treatment of infections more and more difficult. The bactericidal properties of noble metal nanoparticles could be a solution.

In this work silver nanoparticles were produced by using two nanosecond Nd:YVO_4 lasers operating at 1064 and 532 nm respectively to ablate a silver target submerged in pure de-ionized water. Part of the resulting colloidal solution was injected as a fine stream by a compressed air system and re-irradiated one and three times with the same laser to resize and get uniform nanoparticles.

The obtained nanoparticles by ablation and re-irradiation consisted of crystalline Ag nanoparticles with a bimodal size distribution. The particle size has been reduced by subsequent laser re-irradiation with both laser sources, reaching a 40% of mean size reduction. Inhibitory effects on the proliferation of *Staphylococcus aureus* was demonstrated on silver nanoparticles obtained after re-irradiation with the infrared laser.

Keywords: Silver nanoparticles, laser ablation, resizing, antibacterial effects

1. Introduction

It is estimated that by 2050, 10 million persons will die each year due to the resistance of bacteria to antibiotics [1]. This is a huge problem that even today is causing 700.000 fatalities per year. Use of nanoparticles (NPs) could be an alternative to today's antibiotics, since NPs are able to locally destroy bacteria, but preserving the integrity of the surrounding tissues [2].

During the last years, silver nanoparticles have been widely studied because of their antibacterial properties [3-9]. In this way, different studies demonstrated the influence of size and shape of NPs in terms of bactericidal efficacy [7, 10–12]. Therefore, synthesizing nanoparticles with the adequate size distribution, morphology and crystallinity is very important. There are various methods based on physical, chemical or biologic processes to produce silver nanoparticles [13-17]. Obviously each technique has its own pros and cons . Regarding the use as bactericidal agent in human beings, is important to note that most of these methods imply the use of precursors, solvents or involve chemical reactions which can result in the contamination of the obtained nanoparticles, that could be harmful not only to bacteria but also to the surrounding tissues.

Laser ablation of solids in liquids (LASL) allows controlling the size and shape by tuning the processing parameters, but also leading to obtain pure nanoparticles with no need of any additional reagent [18]. In the last decade several groups used this technique for the production of silver NPs [19-24]. Modifications of the original technique such as using a high speed rotating target [25]or a wire target in a liquid jet [26] led to improvements on size of the nanoparticles and on the productivity respectively. With the objective of avoiding any type of contamination, laser ablation of a silver plate was carried out also in open air, obtaining NPs with rounded shape and narrow size distribution [27-28].

In the present work, we report the synthesis of silver nanoparticles by LASL in water using two different laser sources and the subsequent fragmentation of the obtained solutions following a somehow similar strategy as that of Wagener and Barcikowski for producing organic NPs from powders instead of a solid target [29]. In this case, the nanoparticle solutions are irradiated with a focused laser beam at the outlet of a narrow tube to ensure that the optical path of the beam is minimized and the laser beam hits the particles in a fine jet with a reduced thickness. The similar working parameters used by both laser sources together with the experimental configuration, set the ideal conditions to study the effects of the laser wavelength in the ablation and re-irradiation process.

Results and formation process, including influence of wavelength are discussed. Antibacterial activity is also studied with *Staphylococcus aureus* (a gram-positive aerobic bacteria) for being one of the major multidrug-resistant pathogens [9,30], which typically causes skin infections or even pneumonia, endocarditis and osteomyelitis [31].

2. Materials and methods

2.1. Laser Ablation

A silver foil with 99.99% of purity was cleaned and sonicated to be used as laser ablation target. As shown in Figure 1, the target was fixed inside a glass vessel filled with deionized water up to 1mm over the upper surface of the silver foil. The liquid layer thickness selection was made taking into account that this parameter is critical in the NPs formation process. Since the laser fluence in our case is moderate and the laser beam was scanning the substrate, 1mm-thickness layer of liquid above the target was enough to avoid the splash of water drops and to ensure the release of the ablated matter into the surrounding liquid [32].

Two different laser sources working at different wavelengths were used in the process (see Table 1). The first system was a diode-pumped Nd:YVO_4 laser providing pulses of 14 ns at wavelength of 532 nm. The second laser source was a Nd:YVO_4 laser providing pulses of 20 ns at 1064 nm of wavelength. The laser beam spot diameter on the target surface was estimated to be 132 μm giving a fluence of 1.90 J/cm^2 in case of Green laser and 150 μm giving a fluence of 2.03 J/cm^2 for IR laser.

In all experiments, the laser beam was focused on the upper surface of the target and was kept in relative movement with respect to the metallic plate at 50 mm/s of scanning speed The processing time for the LASL was 5 minutes in both cases, taking place a change in the color of the solution, becoming yellowish/brown in the first minutes of the process which evidences the nanoparticle production [33].

2.2. Re-Irradiation

Part of the obtained solutions from the LASL was poured and subjected to pressure to give a horizontal homogeneous and constant stream flowing from a capillary to be re-irradiated once and three times using the same laser sources with the same parameters used for the initial colloidal solution. Table 2 shows the different samples produced and analyzed in this study.

The laser beam was perpendicularly focused on the middle point of the stream at the capillary exit (Fig. 2). The air pressure used during the process was 0.5 bar. This pressure was enough to keep a continuous jet of 0.69 cm^3/s and to assure that laser beam strikes on a homogeneous area.

2.3. Sample preparation and characterization technics

After each experiment, samples of the obtained colloidal suspensions were dropped on carbon-coated copper micro-grids and allowed to dry for characterization with a High-Resolution Transmission Electron Microscopy (HRTEM). Drops of each sample have

been also deposited and dried repeatedly on a glass to get a film with sufficient thickness for the X-ray diffraction (XRD) analysis. The XRD spectra of the samples were compared to that of the starting material.

In order to analyze the particle size, morphology and crystalline structure of the obtained nanoparticles, HRTEM images were obtained using a JEOL-JEM 2010F FEG transmission electron microscope equipped with a slow digital camera scan, using an accelerating voltage of 200 kV and provided with an energy dispersive X-Ray Spectrometer (EDS) to reveal the qualitative elemental composition. The XRD analysis was carried out in order to corroborate the crystal structure by means of a PANanalytical X'Pert Pro X-ray diffractometer using monochromated Cu-Kα radiation (λ= 1.54 Å) over the 30-90º 2θ range with step size of 0.02º. The UV-vis absorption spectrum of the colloidal suspensions was measured in the range from 190 to 800 nm using a Hewlett Packard HP 8452 spectrophotometer. The stability of the colloids was studied by means of the Z-Potential measurements, carried out with a Zetasizer Nano ZS ZEN3600 from Malvern Instruments.

To assess the bactericidal activity of the obtained NPs, the MIC (minimum inhibitory concentration) evaluation was performed with a gram-positive bacteria, *Staphylococcus aureus* subsp. aureus CECT 435 (Colección Española de Cultivos Tipo) using different dilutions (from 1:2 to 1:100) of each colloidal solution with a concentration of 300 mg/L. The growth rates of this bacteria was studied by optical density (OD) measurements. This standard procedure used in microbiology, measures the optical absorbance of a sample at a specific wavelength, to obtain normalized results [34]. The different silver NPs colloids were added (in triplicate) to the wells of a sterile 96-well plate already containing the bacterial suspension in culture media (BHI). To assure homogeneity, the obtained solutions were previously submerged in an ultrasonic bath for 25 minutes at room

temperature. During the assay the plate was incubated at 37 ºC and the absorbance at 600 nm was measured every 15 min for 13 hours using a multimode microplate reader (Infinite 200 PRO, Tecan).

3. Results and discussion

3.1. Size, morphology, composition and crystallography

Figures 3 and 4, show TEM images of Ag nanoparticles obtained with green and IR lasers and their corresponding size distribution. The represented histograms were obtained by measuring the diameter of about 300 particles of each sample.

Note that the silver nanoparticles obtained by LASL with both Green and IR lasers, exhibit rounded shape with certain tendency to agglomeration. This is due to the formation mechanism of nanoparticles and the thermal regime taking place between laser beam and the target. When the laser beam strikes on the Ag foil, the incident radiation is absorbed heating up the silver above its melting point. Because of the high power delivered in the few nanoseconds lasting the laser pulse, the energy density surpasses the ablation threshold of the material and lead to the plasma formation. In water, the plasma plume is confined and it cools down more rapidly than in air [35] forming spherical nanoparticles. Subsequently, the nanoparticles size was reduced by laser re-irradiation. This process causes a large number of small particles as well as a wider range of sizes [36] as can be seen in figures 3 and 4. On account of the metallic nature of the starting material, since although the great majority of the particles are fractured by the laser beam turning out in smaller ones, concurrently the absorbed radiation increases the temperature of the already formed NPs above the melting point, which melt and join with others by coalescence leading to the formation of larger nanoparticles or chains-like nanostructures.

Note that all samples show a bimodal size distribution. In addition, the number of nanoparticles with a diameter lower than 10 nm increased with the re-irradiation times, primarily when the process is carried out with the IR laser.

The influence of laser wavelength on the obtained nanoparticles size and/or concentration can be explained by penetration depth of laser beam, self- absorption, ablation efficiency, etc. It is known that absorption efficiency of the incident laser radiation represents a key parameter in the process. According to previous works, the absorption efficiency of 532 nm for producing Ag nanoparticles is higher than when 1064 nm of wavelength is used [37-38]. This is consistent with TEM images of the nanoparticles obtained directly by the laser ablation of silver target in water, but not with those obtained by re-irradiating the resulted colloidal solutions.

Taking into account thermal evaporation dominates the process of ns ablation [7], nanoparticles fragmentation can be controlled by limiting the interaction zone between the laser beam and nanoparticles on one hand and their interaction time on other hand. Results show that the fragmentation process carried out by using a 1mm-diameter flow, assures that the incident radiation affects a small controlled area, being the laser fluence a parameter of great relevance. Because of the liquid layer surrounding the nanoparticles is very reduced, the high irradiance induces dramatic particles overheating, leading to particles evaporation and explosion. As a result, smaller particles are formed from the fractured ones.

In our results the fragmentation effect is more noticeable in the case IR wavelength due to its higher fluence. Similar results have been reported in previous works, showing that particle size decrease by increasing the pulse fluence [38, 36].

The EDS performed on each obtained sample confirms that the as-ablated as well as the re-irradiated nanoparticles are pure Ag. Moreover, all the particles obtained, even the

smallest ones are crystalline. This aspect can be observed in Figure 5, showing HRTEM of single nanoparticles with clear lattice fringes and their corresponding Fast Fourier Transform (FFT) as insets.

To elucidate the crystalline phases of the obtained Ag nanoparticles, the measured interplanar distances from the FFT were compared with those of metallic Ag in Table 3. The measured interplanar distances correspond with the family planes of cubic Ag (JCPDS-ICDD ref.00-004-0783). Note that the composition seems to be not modified in the process.

In order to corroborate the composition of the obtained nanoparticles, XRD were performed on the obtained nanoparticles and the precursor silver plate. The corresponding comparative diffraction patterns of the samples are depicted in Figure 6. As can be seen from Fig. 6 the crystalline phase of the obtained nanoparticles is not altered by the re-irradiation process, changing only size and shape.

As shown in Fig. 7a, the UV-VIS spectra of the synthesized nanoparticles exhibit a peak at approximately 400nm, which is characteristic of surface plasmon resonance (SPR) feature of Ag nanoparticle colloidal solutions [36]. The SPR is a well-known metallic nanoparticles effect, since it is absent in individual atoms and in metallic bulk. It is associated to the nanoparticles shape, size and surrounding medium in a way that the presence of a single surface plasmon peak, implies that they are spherical [36-37]. The pronounced peak corresponds to the as-ablated nanoparticles while the broadening in the re-irradiated ones is characteristic of a wide size distribution [40] which is in agreement with the TEM observations.

Measurements of absorbance of each sample were repeated after 14 days. As shown in Fig. 7b, the single surface plasmon peak of as-ablated nanoparticles has slightly blue-shifted. This effect, although implies that they are still spherical could be attributed to the

presence of silver oxide on the AgNPs [7]. In addition, the absorbance peak of the samples obtained by re-irradiation with both lasers have been softened, which could be indicative of the agglomeration.

3.2. Colloid stability

It is known that colloid stability depends on the interactions between its particles in suspension which in turn are the result of electrostatic repulsive forces and Van der Waals attractive forces [39, 41]. The electrokinetic potential, commonly known as Zeta potential (ZP) provides information about the interactions that take place through the measurement of the particles speed under the influence of an electric field applied.

As shown in Table 4, the measurements show a higher (absolute value) potential for the particles obtained by laser ablation than the re-irradiated particles, decreasing with the number of times the sample is re-processed. In this sense, guidelines confer higher instability for colloidal solutions with low ZP values (below 10 mV) than others with values around 20 mV. In addition, all values are negative, which reveals a basic pH [41] of a great importance in biological applications.

Measurements were repeated after 14 days (Table 5) showing similar values to those initially obtained, with a slight tendency to reduce the ZP values in time, but preserving certain stability.

This stability is also confirmed by means of the colloids color, since after 14 days the colloidal solutions preserve their yellowish-brown tonality. This is especially significative for the initial colloids, because of the NPs are suspended by the repulsive force exerted among them, while NPs obtained by means of the re-irradiation process (with lower ZP values) tend towards agglomeration looking for a more stable equilibrium condition. This balance between the particles, is known as total interaction potential which depends among others, on the electrolyte concentration, the valence of counterions,

as well as the particle size [42], being larger particles less probable to coagulate than smaller particles [43].

3.3. Analysis of antimicrobial activity

Antimicrobial activity of the obtained solutions was evaluated through standard Optical Density measurements at wavelength of 600nm (OD600). Due to the different absorbance at 600 nm of each solution before being added to the culture medium, the relative values (to the initial absorbance value) were calculated for comparing the results. Only the 1:2 dilution showed antibacterial effects. The obtained relative absorbance of each sample is shown in Fig. 8.

Taking into account that this method measures the turbidity of bacterial suspensions by means of its absorbance, stablishing that the higher the absorbance, the more bacterial concentration [34]. Values were compared with a positive and a negative control (medium with bacteria but without NPs and medium without bacteria respectively). After 13 h the bacterial growth values are noteworthy reduced in all samples. Silver nanoparticles obtained by re-irradiation once, exhibit a greater bactericidal capacity than their precursors (as ablated), being samples b.1 and b.2 those that show the most remarkable inhibitory effects. The rest of curves show a delay in the growth, after which the bacterial proliferation starts.

Earlier studies [5,11,44] have demonstrated that Ag NPs with a size between 1 and 10 nm are the ones with the greatest bactericidal effects. In this study, the smallest nanoparticles which correspond with sample a.3 do not show the best inhibitory effects because of the formation of agglomerates, resulting in a decrease of Ag^+ ions release [45], the main responsible for bacterial inhibition [4,46]. Which seems to indicate that the electrolyte

concentration of this sample at the beginning is too high and the coagulation takes place very fast.

Note that the samples with the highest bactericidal effect (b.2, b.1 y a.2), correspond to those that underwent a greater variation in their ZP values after 14 days.

This results are consistent with works previously reported and demonstrate not only the influence of size, but also morphology and stability of colloidal Ag NPs in the bactericidal effects [10,47]. In this sense, the addition of salts to the solution before irradiation, would prevent the formation of agglomerates and improve the stability of the NPs in colloidal suspension [48]. In order to improve the method, further research will be carried out in this direction.

4. Conclusions

Feasibility of a small-diameter flow to reduce the size of silver nanoparticles by laser radiation is demonstrated. Crystalline Ag nanoparticles have been obtained by means of LASL and re-irradiation technique using two different nanosecond Nd:YVO_4 lasers working at 532 nm and 1064 nm of wavelength, without any chemical reagent or contamination. The particles obtained by LASL exhibit rounded shape. After re-irradiation, nanoparticle size is reduced, nevertheless part of the fractured particles coalescence leading to the formation of larger nanoparticles or chains-like nanostructures with a wide range of sizes. All particles show very strong tendency to agglomeration. This is consistent with the metallic nature of the material and the thermal formation mechanisms.

Despite the fact that both wavelengths reduce the average size of the nanoparticles by means of the re-irradiation process, the number of particles with a diameter smaller than 10nm increases considerably if the wavelength used is 1064 nm.

The antibacterial study showed that *s. aureus* is susceptible to the obtained silver nanoparticles, reaching the best inhibitory effects those nanoparticles obtained by laser ablation and re-irradiation with 1064 nm of wavelength. This result confirms the influence of size, shape and stability in the bactericidal effects of silver nanoparticles.

Acknowledgements

This work was partially supported by the EU research project CVmar+i (INTERREG V A España-Portugal (POCTEP), by the Government of Spain (MAT2015-71459-C2-P (MINECO/FEDER), PRX17/00157) and by Xunta de Galicia ((ED431B 2016/042, ED481D 2017/010, ED481B 2016/047-0). Miguel A. Correa-Duarte together with his Investigations Group TeamNanoTech (CINBIO) and the technical staff from CACTI (University of Vigo) are gratefully acknowledged.

References

[1] J. O'Neil, The Review on Antimicrobial Resistance – Tackling drug resistant infections globally: Final report and recommendations, (2016). Electronic version can be find at https://amr-review.org/ web page.

[2] M.J. Hajipour, K.M. Fromm, A.A. Ashkarran, D.J. de Aberasturi, I.R.de Larramendi, T. Rojo, V. Serpooshan, W.J. Parak, M. Mahmoudi, Antibacterial properties of nanoparticles. Trends in Biotechnology, 30 (2012) 499–511.

[3] I. Sondi, B. Salopek-Sondi, Silver nanoparticles as antimicrobial agent: a case study on E. coli as a model for Gram-negative bacteria. Journal of Colloid and Interface Science 275 (2004) 177–182.

[4] A. Petica, S. Gavriliu, M. Lungu, N. Buruntea, C. Panzaru, Colloidal silver solutions with antimicrobial properties, Mater. Sci. Eng. B Solid-State Mater. Adv. Technol. 152 (2008) 22–27. doi:10.1016/j.mseb.2008.06.021.

[5] S. Chernousova, M. Epple, Silver as antibacterial agent: Ion, nanoparticle, and metal, Angew. Chemie - Int. Ed. 52 (2013) 1636–1653. doi:10.1002/anie.201205923.

[6] S. Pal, Y.K. Tak, J.M. Song, Does the antibacterial activity of silver nanoparticles depend on the shape of the nanoparticle? A study of the gram-negative bacterium Escherichia coli, J. Biol. Chem. 290 (2015) 1712–1720. doi:10.1128/AEM.02218-06.

[7] B. Perito, E. Giorgetti, P. Marsili, M. Muniz-Miranda, Antibacterial activity of silver nanoparticles obtained by pulsed laser ablation in pure water and in chloride solution, Beilstein J. Nanotechnol. 7 (2016) 465–473. doi:10.3762/bjnano.7.40.

[8] M. Ratti, J.J. Naddeo, Y. Tan, J.C. Griepenburg, J. Tomko, C. Trout, S.M. O'Malley, D.M. Bubb, E.A. Klein, Irradiation with visible light enhances the antibacterial toxicity of silver nanoparticles produced by laser ablation, Appl. Phys. A. 122 (2016) 346. doi:10.1007/s00339-016-9935-8.

[9] Y.G. Yuan, Q.L. Peng, S. Gurunathan, Effects of silver nanoparticles on multiple drug-resistant strains of Staphylococcus aureus and Pseudomonas aeruginosa from mastitis-infected goats: An alternative approach for antimicrobial therapy, Int. J. Mol. Sci. 18 (2017). doi:10.3390/ijms18030569.

[10] C. Marambio-Jones, E.M.V. Hoek, A review of the antibacterial effects of silver nanomaterials and potential implications for human health and the environment, J. Nanoparticle Res. 12 (2010) 1531–1551. doi:10.1007/s11051-010-9900-y.

[11] M. Guzman, J. Dille, S. Godet, Synthesis and antibacterial activity of silver nanoparticles against gram-positive and gram-negative bacteria, Nanomedicine Nanotechnology, Biol. Med. 8 (2012) 37–45. doi:10.1016/j.nano.2011.05.007.

[12] J.W. Rhim, L.F. Wang, Y. Lee, S.I. Hong, Preparation and characterization of bio-nanocomposite films of agar and silver nanoparticles: Laser ablation method, Carbohydr. Polym. 103 (2014) 456–465. doi:10.1016/j.carbpol.2013.12.075.

[13] A. Panacek, L. Kvítek, R. Prucek, M. Kolár, R. Vecerová, N. Pizúrová, V.K. Sharma, T. Nevecna, R. Zboril. Silver Colloid Nanoparticles: Synthesis, Characterization, and Their Antibacterial Activity, J. Phys. Chem. B (2006) 16248–16253.

[14] K.H. Tseng, Y.C. Chen, J.J. Shyue, Continuous synthesis of colloidal silver nanoparticles by electrochemical discharge in aqueous solutions, J. Nanopart. Res. 13 (2011) 1865–1872.

[15] M.N. Nadagouda, T.F. Speth, R.S. Varma, Microwave-assisted green synthesis of silver nanostructures, Acc. Chem. Res. 44 (2011) 469–478.

[16] J.L. López-Miranda, M. Vázquez, N. Fletes, R. Esparza, G. Rosas, Biosynthesis of silver nanoparticles using a Tamarix gallica leaf extract and their antibacterial activity, Mater. Lett. 176 (2016) 285–289.

[17] I. Ghiuță, D. Cristea, C. Croitoru, J. Kost, R. Wenkert, I. Vyrides, A. Anayiotos, D. Munteanu, Characterization and antimicrobial activity of silver nanoparticles, biosynthesized using Bacillus species, Appl. Surf. Sci. 438 (2017) 66–73. doi:10.1016/j.apsusc.2017.09.163.

[18] S. Barcikowski, G. Compagnini, Advanced nanoparticle generation and excitation by lasers in liquids, Phys.Chem. Chem. Phys., 15 (2013) 3022.

[19] S. Barcikowski, S., A. Méndez-Manjón, B. Chichkov, M. Brikas, G. Raciukaitis, Generation of nanoparticle colloids by picosecond and femtosecond laser ablations in liquid flow, Appl. Phys. Lett. 91 (2007), 083113.

[20] B. Xu, R.G. Song, Fabrication of Ag nanoparticles colloids by pulsed laser ablation in liquid, Avanced Materials Research, 123-125 (2010) 675–678.

[21] M.I. Mendivil, B. Krishnan, F.A. Sánchez, S. Martínez, J.A. Aguilar-Martínez, G.A. Castillo, D.I. García-Gutiérrez, S. Shaji, Synthesis of silver nanoparticles and antimony oxide nanocrystals by pulsed laser ablation in liquid media, Appl Phys A 110 (2013) 809–816.

[22] S.V. Rao, G.K. Podagatlapalli, S. Hamad, Ultrafast laser ablation in liquids for nanomaterials and applications, J. Nanosci Nanotechnol. 14 (2014) 1364–1388.

[23] M.A. Valverde-Alva, T. García-Fernández, M. Villagrán-Muniz, C. Sánchez-Aké, R. Castañeda-Guzmán, E. Esparza-Alegría, C.F. Sánchez-Valdés, J.L.S. Llamazares, C.E.M. Herrera, Synthesis of silver nanoparticles by laser ablation in ethanol: A pulsed photoacoustic study, Appl. Surf. Sci. 355 (2015) 341–349.

[24] M. Dell'Aglio, V. Mangini, G. Valenza, O. De Pascale, A. De Stradis, G. Natile, G.,F. Arnesano, A. De Giacomo, Silver and gold nanoparticles produced by pulsed laser ablation in liquid to investigate their interaction with Ubiquitin, Appl. Surf. Sci., 374 (2016) 297–304.

[25] A. Resano-García, S. Champmartin, Y. Battie, A. Koch, A. En Naciri, A. Ambari, N. Chaoui, Highly-repeatable generation of very small nanoparticles by pulsed-laser ablation in liquids of a high-speed rotating target, Phys.Chem.Chem.Phys., 18 (2016) 32868.

[26] S. Kohsakowski, A. Santagata, M. Dell'Aglio, A. de Giacomo, S. Barcikowski, P. Wagener, B. Gökce, High productive and continuous nanoparticle fabrication by laser ablation of a wire-target in a liquid jet, Appl. Surf. Sci. 403 (2017) 487–499.

[27] M. Boutinguiza, R. Comesaña, F. Lusquiños, A. Riveiro, J. Del Val, J. Pou, Production of silver nanoparticles by laser ablation in open air, Appl. Surf. Sci. 336 (2015) 108–111. doi:10.1016/j.apsusc.2014.09.193.

[28] M. Boutinguiza, M. Fernández-Arias, J. del Val, J. Buxadera-Palomero, D. Rodríguez, F. Lusquiños, F.J. Gil, J. Pou, Synthesis and deposition of silver nanoparticles on cp Ti by laser ablation in open air for antibacterial effect in dental implants, Mater. Lett. 231 (2018) 126–129. doi:10.1016/j.matlet.2018.07.134.

[29] P. Wagener, S. Barcikowski, Laser fragmentation of organic microparticles into colloidal nanoparticles in a free liquid jet, Appl Phys A 101 (2010) 435–439.

[30] R. Salomoni, P. Léo, M.F.A. Rodrigues, Antibacterial Activity of Silver Nanoparticles (AgNPs) in Staphylococcus aureus and Cytotoxicity Effect in Mammalian Cells, Battle Against Microb. Pathog. Basic Sci. Technol. Adv. Educ. Programs. (2015) 851–857.

[31] D.S. Ondusko, D. Nolt, Staphylococcus aureus, Pediatr. Rev. 39 (2018) 287–298. doi:10.1542/pir.2017-0224.

[32] T.T. Phuong Nguyen, R. Tanabe-Yamagishi, Y. Ito (in press), Impact of liquid layer thickness on the dynamics of nano- to sub-microsecond phenomena of nanosecond

pulsed laser ablation in liquid, Appl. Surf. Sci. (2018). doi:10.1016/j.apsusc.2018.10.160.

[33] C.G. Moura, R.S.F. Pereira, M. Andritschky, A.L.B. Lopes, J.P. de F. Grilo, R.M. do Nascimento, F.S. Silva, Effects of laser fluence and liquid media on preparation of small Ag nanoparticles by laser ablation in liquid, Opt. Laser Technol. 97 (2017) 20–28. doi:10.1016/j.optlastec.2017.06.007.

[34] S. McBirney, K. Trinh, A. Wong-Beringer, A. Armani, Wavelength-normalized spectroscopic analysis of Staphylococcus aureus and Pseudomonas aeruginosa growth rates, Biomed. Opt. Express. 7 (2016) 4034–4042.

[35] F. Luo, Y. Guan, W. Ong, Z. Du, G. Ho, F. Li, S. Sun, G. Lim, M. Hong, Enhancement of pulsed laser ablation in environmentally friendly liquid, Opt. Express. 22 (2014) 23875. doi:10.1364/OE.22.023875.

[36] J. Jeon, S. Yoon, H.W. Choi, J. Kim, D. Farson, The Effect of Laser Pulse Widths on Laser — Ag Nanoparticle Interaction : Femto- to Nanosecond Lasers, Appl. Sci. 8 (2018) 13. doi:10.3390/app8010112.

[37] A. Pyatenko, H. Wang, N. Koshizaki, T. Tsuji, Mechanism of pulse laser interaction with colloidal nanoparticles, Laser Photonics Rev. 9 (2013) 1–9. doi:10.1002/lpor.201300013.

[38] J. Hajiesmaeilbaigi, F. Mohammadalipour, A. Sabbaghzadeh, S. Hoseinkhani, H.R. Fallah, Preparation of silver nanoparticles by laser ablation and fragmentation in pure water, Laser Phys. Lett. 3 (2006) 252–256. doi:10.1002/lapl.200510082.

[39] V. Amendola, M. Meneghetti, Laser ablation synthesis in solution and size manipulation of noble metal nanoparticles, (2009) 3805–3821. doi:10.1039/b900654k.

[40] S. Dadras, M.J. Torkamany, P. Jafarkhani, Analysis and optimization of silver nanoparticles laser synthesis with emission spectroscopy of induced plasma, J. Nanosci. Nanotechnol. 12 (2012) 3115–3122. doi:10.1166/jnn.2012.5830.

[41] S. Bhattacharjee, DLS and zeta potential – What they are and what they are not?, J. Control. Release. 235 (2016) 337–351. doi:10.1016/j.jconrel.2016.06.017.

[42] J.L. Arias, M. López-Viota, M.A. Ruiz, Ultrasmall superparamagnetic iron oxide particles for biomedical applications, Ars Pharm. 49 (2008) 101–111.

[43] B. Liu, Effect of particle size on critical coagulation concentration, J. Colloid Interface Sci. 198 (1998) 186–189. doi:10.1006/jcis.1997.5275.

[44] J.R. Morones, J.L. Elechiguerra, A. Camacho, K. Holt, J.B. Kouri, J.T. Ramírez, M.J. Yacaman, The bactericidal effect of silver nanoparticles, Nanotechnology. 16 (2005) 2346–2353. doi:10.1088/0957-4484/16/10/059.

[45] G. V. Vimbela, S.M. Ngo, C. Fraze, L. Yang, D.A. Stout, Antibacterial properties and toxicity from metallic nanomaterials, Int. J. Nanomedicine. 12 (2017) 3941–3965. doi:10.2147/IJN.S134526.

[46] Z.M. Xiu, Q.B. Zhang, H.L. Puppala, V.L. Colvin, P.J.J. Alvarez, Negligible particle-specific antibacterial activity of silver nanoparticles, Nano Lett. 12 (2012) 4271–4275. doi:10.1021/nl301934w.

[47] N. Sheikh, A. Akhavan, M.Z. Kassaee, Synthesis of antibacterial silver nanoparticles by γ-irradiation, Phys. E Low-Dimensional Syst. Nanostructures. 42 (2009) 132–135. doi:10.1016/j.physe.2009.09.013.

[48] C. Rehbock, V. Merk, L. Gamrad, R. Streubel, S. Barcikowski, Size control of laser-fabricated surfactant-free gold nanoparticles with highly diluted electrolytes and their subsequent bioconjugation. Phys.Chem. Chem. Phys., 2013, 15, 3057.

Figure captions

Fig. 1. Laser ablation process

Fig. 2. Pressurized air system scheme

Fig. 3. TEM micrographs and size distribution of Ag nanoparticles obtained in water using a Nd:YVO_4 laser operating at 532 nm. a.1) after laser ablation of Ag foil, a.2) after one re-irradiation, a.3) after 3 re-irradiations.

Fig.4. TEM micrographs and size distribution of Ag nanoparticles obtained in water using a Nd:YVO_4 laser operating at 1064 nm. b.1) after laser ablation of Ag foil, b.2) after one re-irradiation, b.3) after 3 re-irradiations.

Fig.5. HRTEM images and their corresponding FFT of Ag crystalline nanoparticles obtained in water using a Nd:YVO_4 laser operating at 1064 nm. b.1) by laser ablation of Ag foil and b.3) after 3 re-irradiations.

Fig.6. XRD of Ag nanoparticles obtained with a wavelength of 532 nm by: a.1) LASL, a.2) re-irradiation 1 time, a.3) re-irradiation 3 times and with 1064 nm of wavelength by: b.1) LASL, b.2) re-irradiation 1 time, b.3) re-irradiation 3 times.

Fig.7a. UV-vis spectrum of Ag nanoparticles obtained with a wavelength of 532 nm by: a.1) LASL, a.2) re-irradiation 1 time, a.3) re-irradiation 3 times and with 1064 nm of wavelength by: b.1) LASL, b.2) re-irradiation 1 time, b.3) re-irradiation 3 times.

Fig.7b. UV-vis spectrum of Ag nanoparticles obtained after 14 days.

Fig.8. Growth curves of *S. aureus* with dilution of 1:2 during 13 h of incubation at 37 ºC in contact with the colloids. Bacterial suspension in the absence of NPs were used as positive control (C+) and medium without bacteria as negative control (C-).

Figure 1

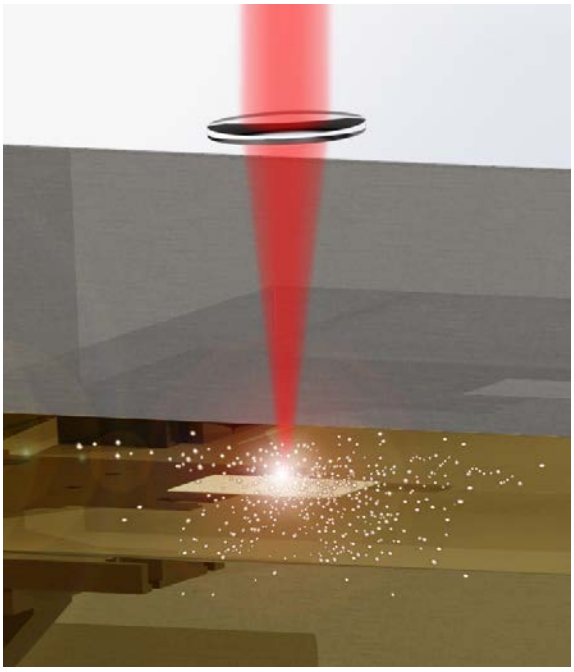

Figure 2

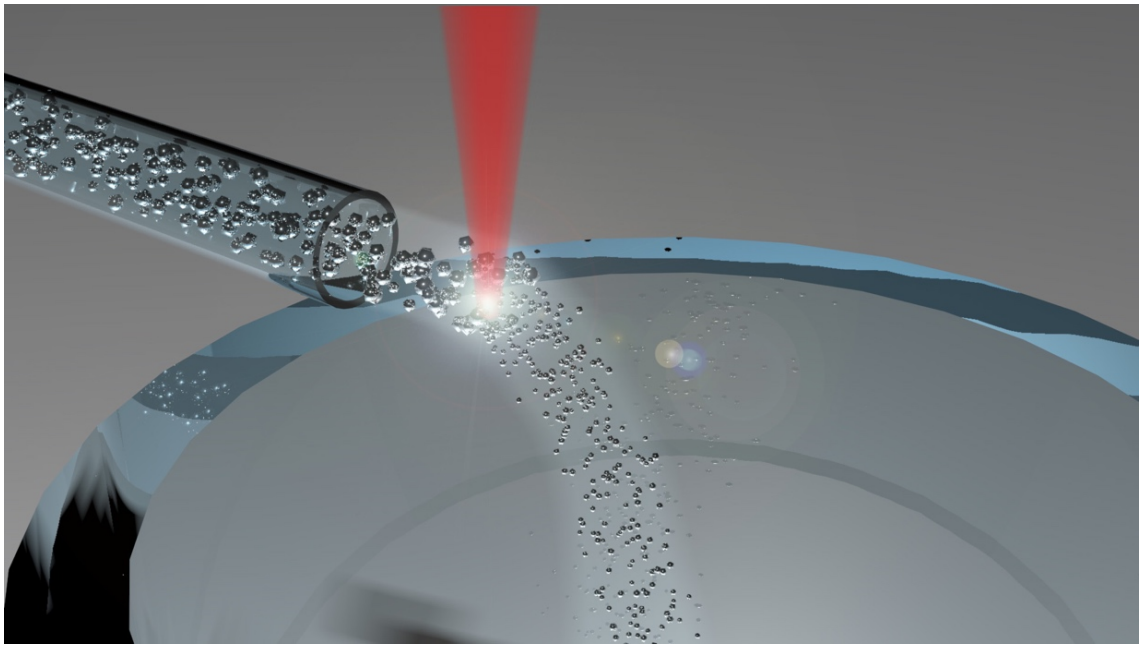

Figure 3

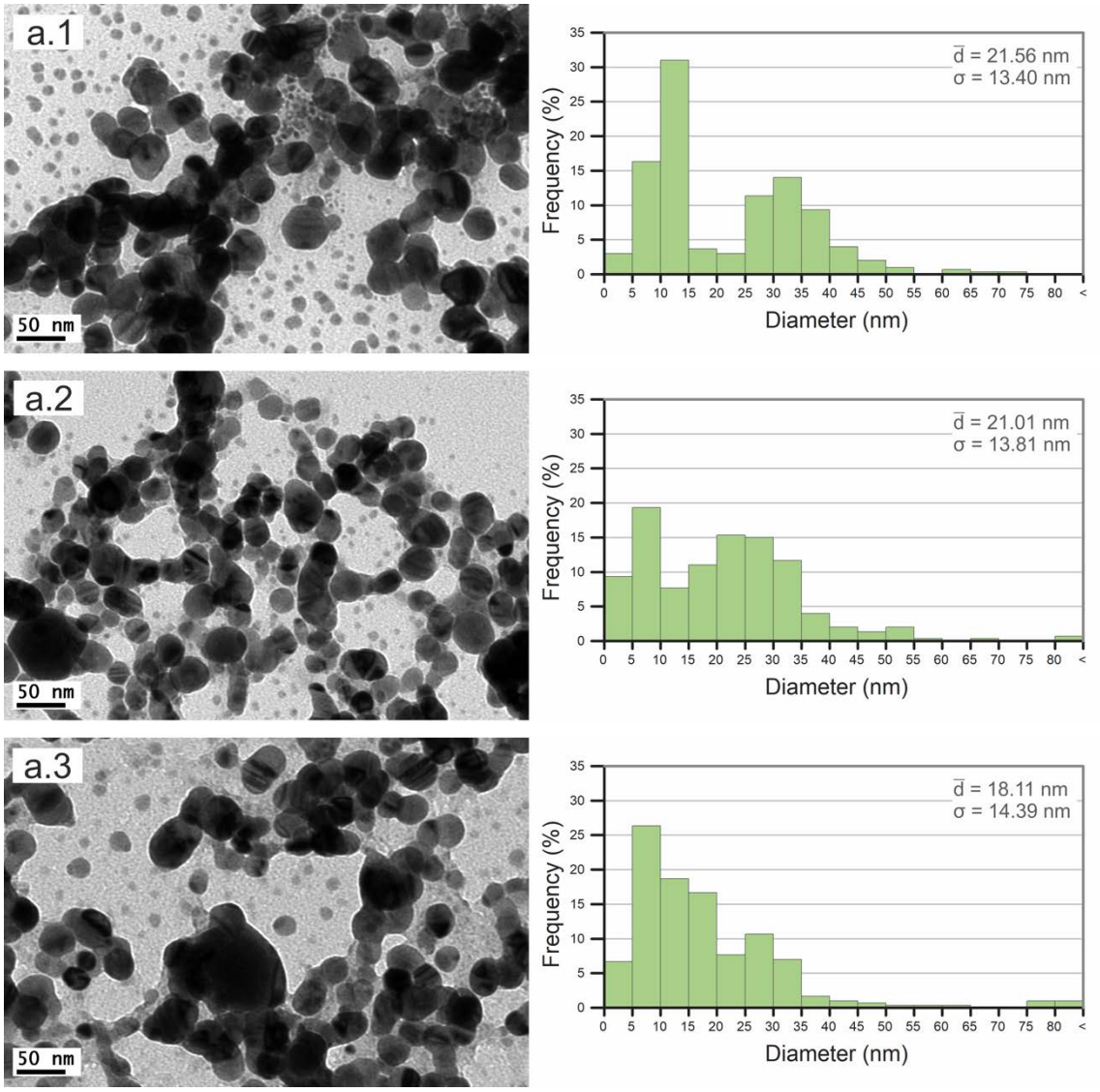
a.1
50 nm
d̄ = 21.56 nm
σ = 13.40 nm
Frequency (%)
Diameter (nm)
a.2
50 nm
d̄ = 21.01 nm
σ = 13.81 nm
Frequency (%)
Diameter (nm)
a.3
50 nm
d̄ = 18.11 nm
σ = 14.39 nm
Frequency (%)
Diameter (nm)

Figure 4

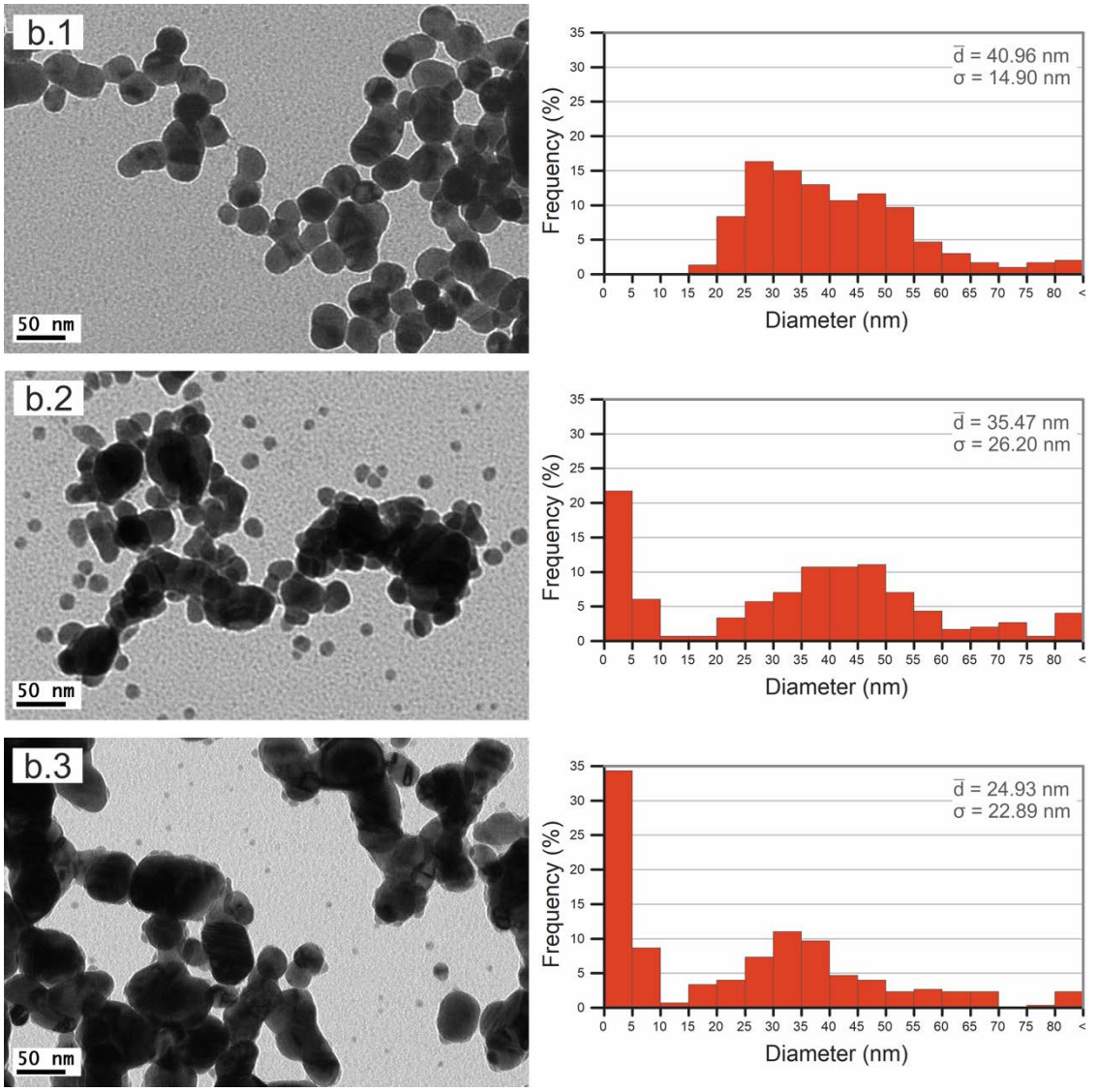
b.1
50 nm
d̄ = 40.96 nm
σ = 14.90 nm
Frequency (%)
Diameter (nm)
b.2
50 nm
d̄ = 35.47 nm
σ = 26.20 nm
Frequency (%)
Diameter (nm)
b.3
50 nm
d̄ = 24.93 nm
σ = 22.89 nm
Frequency (%)
Diameter (nm)

Figure 5

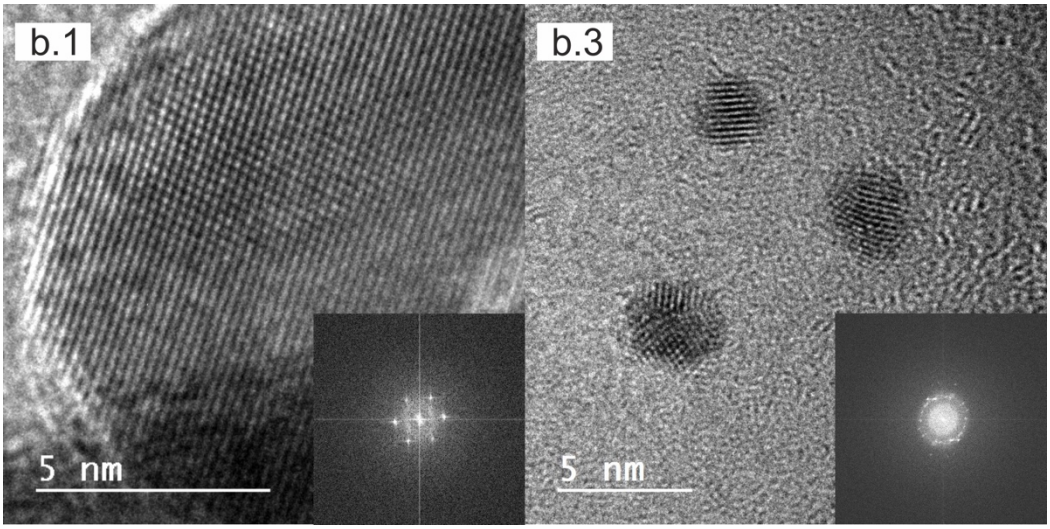

Figure 6

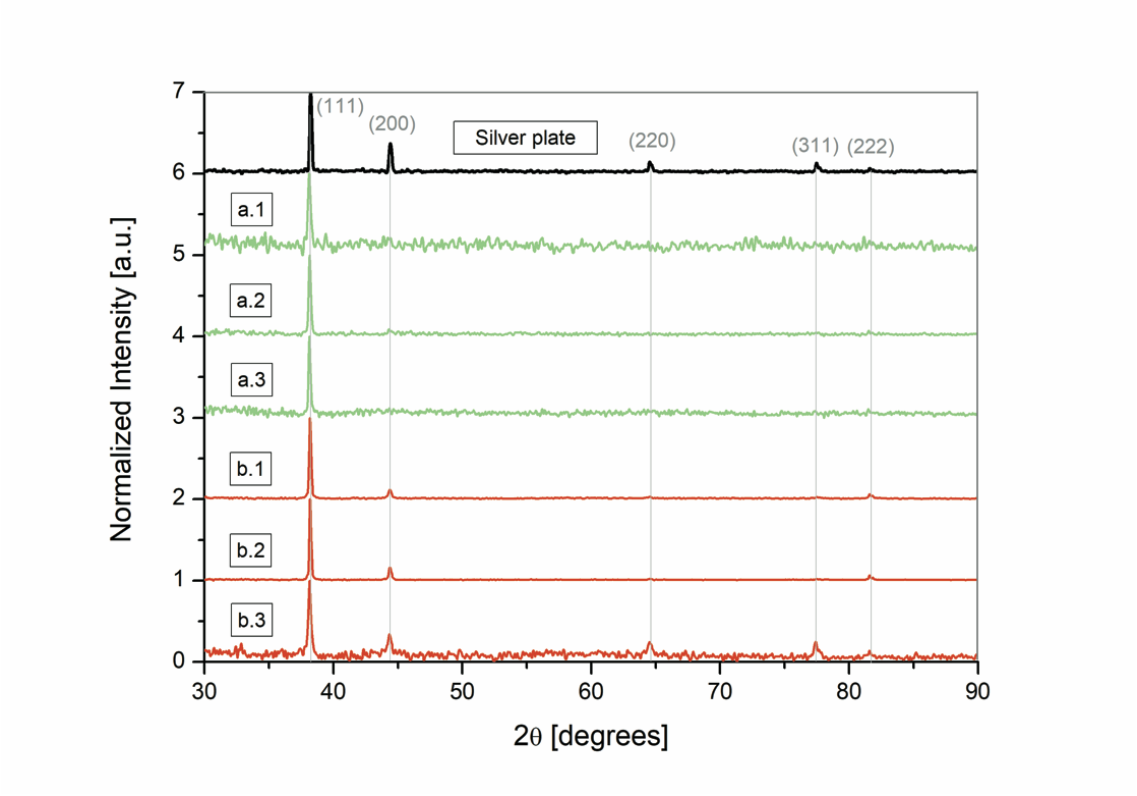
Normalized Intensity [a.u.]
2θ [degrees]
(111)
(200)
Silver plate
(220)
(311)
(222)
a.1
a.2
a.3
b.1
b.2
b.3
0
1
2
3
4
5
6
7
30
40
50
60
70
80
90

Figure 7a

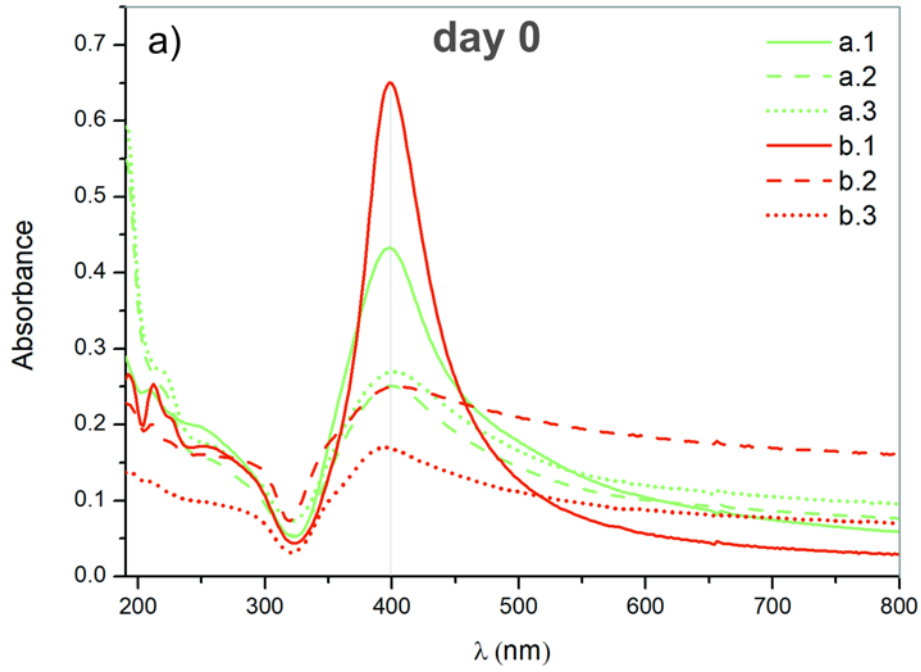
a)
day 0
a.1
a.2
a.3
b.1
b.2
b.3
Absorbance
λ (nm)
0.0
0.1
0.2
0.3
0.4
0.5
0.6
0.7
200
300
400
500
600
700
800

Figure 7b

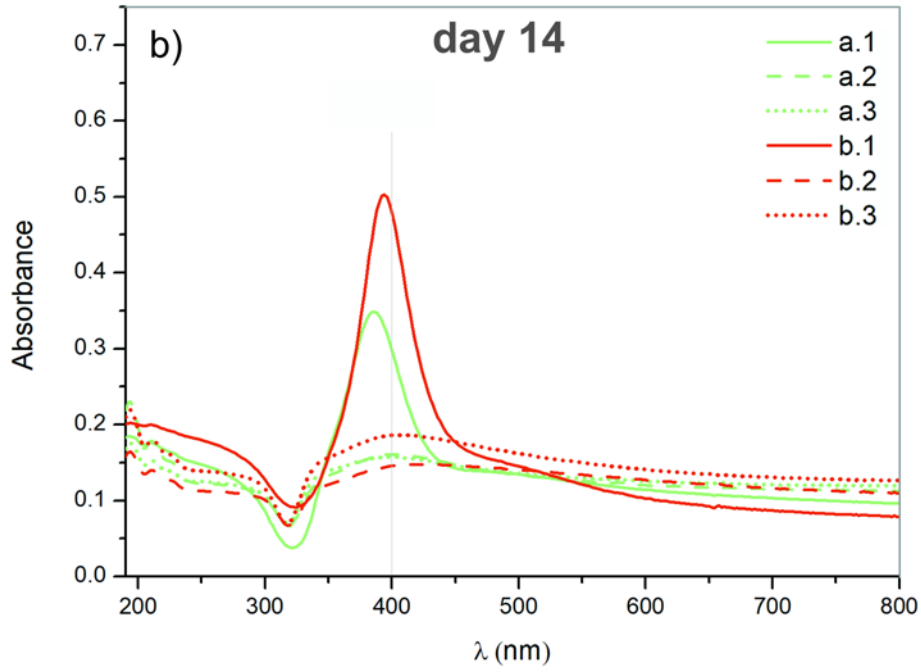
b)
day 14
a.1
a.2
a.3
b.1
b.2
b.3
Absorbance
λ (nm)
0.0
0.1
0.2
0.3
0.4
0.5
0.6
0.7
200
300
400
500
600
700
800

Figure 8

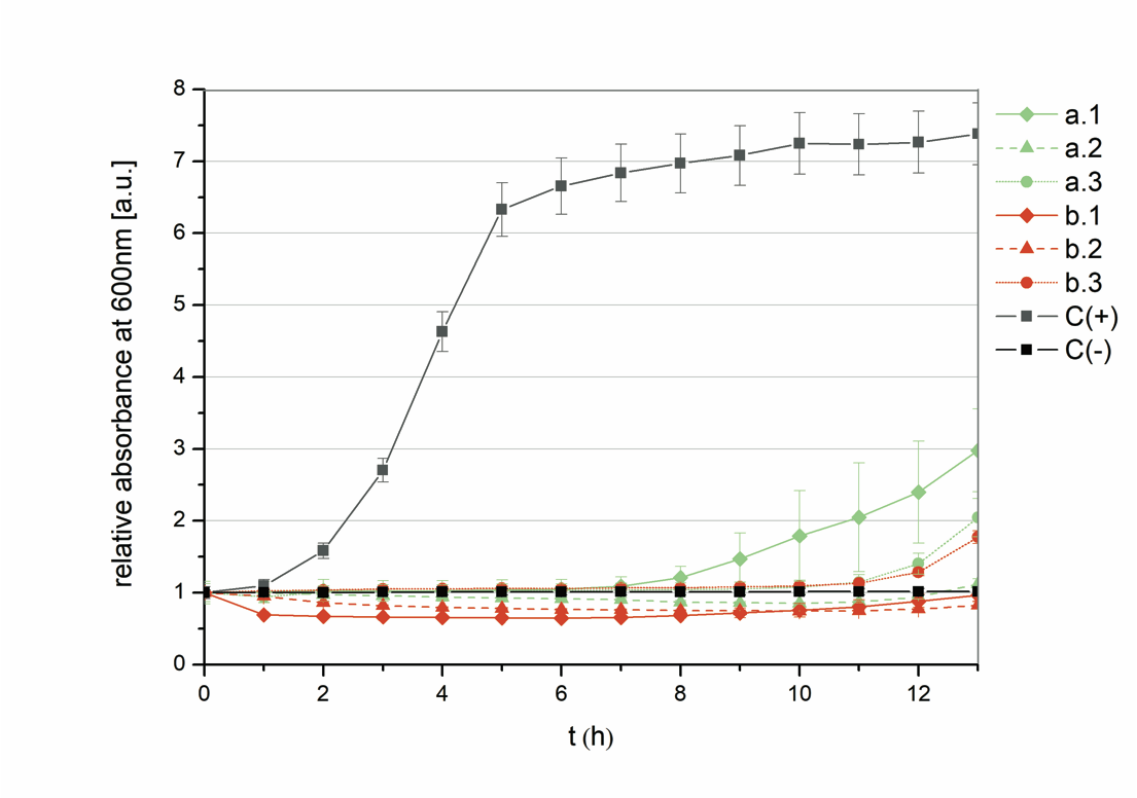

Table 1. Processing parameters

Laser source		Wavelength (nm)	Pulse length (ns)	Frequency (kHz)	Energy density (J/cm^2)	Scanning speed (mm/s)
Laser	Green	532	14	20	1.90	50
	IR	1064	20	20	2.03	50

Table 2. Set of samples produced and analyzed

Sample	Laser source	Treatment
a.1	Green	As produced
a.2	Green	1 time re-irradiation
a.3	Green	3 times re-irradiation
b.1	IR	As produced
b.2	IR	1 time re-irradiation
b.3	IR	3 times re-irradiation

Table 3. Lattice spacing measured from the FFT of Ag nanoparticles obtained by a.1), b.1) laser ablation, a.2), b.2) by one re-irradiation, a.3), b.3) by 3 re-irradiations, using 532 nm and 1064 nm respectively and compared to those of metallic Ag.

a.1	a.2	a.3	b.1	b.2	b.3	Ag (hkl)
0.236	0.234	0.235	0.235	0.239	0.233	0.2359 (1 1 1)
0.209	0.208	0.214	0.192	0.222	0.201	0.2044 (2 0 0)
-	-	-	0.155	-	0.137	0.1445 (2 2 0)
-	0.116	-	-	-	-	0.11796 (2 2 2)

Table 4. Z-Potential measurements

Sample	a.1	a.2	a.3	b.1	b.2	b.3
Z Potential (mV) day 0	-23.5	-9.18	-1.90	-19.03	-19.33	-11.5
Z Potential (mV) day 14	-21.73	-5.40	-1.75	-15.77	-15.03	-11.5

Highlights

- Ag nanoparticles (NPs) size is reduced by laser re-irradiating a NPs thin flow.
- Composition and crystal structure are not modified in the re-irradiation process.
- The obtained NPs show remarkably bactericidal effects after 13 hours.
- The re-irradiation process improves the antibacterial properties of the NPs.

Graphical Abstract